THROMBOSIS AND HEMOSTASIS

Vascular Gas6 contributes to thrombogenesis and promotes tissue factor up-regulation after vessel injury in mice

*Richard S. Robins,[1] *Catherine A. Lemarié,[1] Sandrine Laurance,[1] Meghedi N. Aghourian,[1] Jianqiu Wu,[1,2] and Mark D. Blostein[1]

[1]Lady Davis Institute for Medical Research, and [2]Department of Medicine, Jewish General Hospital, McGill University, Montreal, QC

Key Points

- The present study shows, for the first time, that Gas6 produced by endothelial cells contributes to venous thrombus formation.
- Gas6 is required for the expression of tissue factor in endothelial cells.

Gas6 (growth-arrest specific gene 6) plays a role in thrombus stabilization. *Gas6* null (−/−) mice are protected from lethal venous and arterial thromboembolism through platelet signaling defects induced only by 5μM ADP and 10μM of the thromboxane analog, U46619. This subtle platelet defect, despite a dramatic clinical phenotype, raises the possibility that Gas6 from a source other than platelets contributes to thrombus formation. Thus, we hypothesize that Gas6 derived from the vascular wall plays a role in venous thrombus formation. Bone marrow transplantation and platelet depletion/reconstitution experiments generating mice with selective ablations of Gas6 from either the hematopoietic or nonhematopoietic compartments demonstrate an approximately equal contribution by Gas6 from both compartments to thrombus formation. Tissue factor expression was significantly reduced in the vascular wall of *Gas6*$^{-/-}$ mice compared with WT. In vitro, thrombin-induced tissue factor expression was reduced in *Gas6*$^{-/-}$ endothelial cells compared with wild-type endothelium. Taken together, these results demonstrate that vascular Gas6 contributes to thrombus formation in vivo and can be explained by the ability of Gas6 to promote tissue factor expression and activity. These findings support the notion that vascular wall-derived Gas6 may play a pathophysiologic role in venous thromboembolism. (*Blood*. 2013;121(4):692-699)

Introduction

Venous thromboembolism (VTE) is a common cause of morbidity and mortality in clinical medicine. The pathophysiology of VTE was first described by Virchow in 1853 and describes a triad of entities accounting for VTE. VTE could be triggered by alterations in the blood composition (thrombophilia), changes in blood flow (eg, stasis), and/or activation of the endothelium.[1] Under normal conditions, the endothelial surface inhibits coagulation because of the presence of various proteins, such as tissue factor (TF) pathway inhibitor, thrombomodulin, and the endothelial cell protein C receptor.[2] However, physical (eg, vascular damage) or functional (eg, hypoxia) perturbation of the endothelium promotes thrombosis because of reduced expression of anticoagulants and the induction of the expression of the transmembrane procoagulant protein TF.[3]

Gas6, the product of growth arrest specific gene 6 (*Gas6*), is a member of the vitamin K-dependent family of proteins, which includes the procoagulant factors II, VII, IX, and X and the anticoagulant factors, protein C and S, as well as protein Z.[4] Even though Gas6 was discovered as a homolog of protein S more than a decade ago, it plays no role in the generation of fibrin and its role in vivo remains incompletely characterized.[5,6]

Originally identified in fibroblasts, Gas6 is expressed in various cell types, including endothelial cells,[7] smooth muscle,[8] and bone marrow cells.[9] Gas6 is a ligand for the TAM family of receptor tyrosine kinases, which include Axl, Tyro3 (Sky), and Mer.[10] Gas6 has been shown to have a wide range of biologic functions that is reflected by a broad tissue expression profile. For example, Gas6 is found in plasma[11] as well as in hepatic,[12] renal,[13] and neural tissues.[14,15] Gas6 and its receptors modify platelet activation and aggregation,[16,17] but the role of Gas6 in the interplay between platelets and other cell types, such as endothelial cells, remains unclear. In vivo, *Gas6*-deficient mice are protected from lethal thromboembolism, suggesting a prothrombotic role for Gas6.[16] This antithrombotic phenotype results from a loss of platelet signaling with consequent clot instability. Interestingly, these mice did not have a bleeding diathesis. Platelets from *Gas6*$^{-/-}$ mice showed defective platelet signaling when challenged with 5μM ADP or with 10μM of the thromboxane analog U46619 but not to other platelet agonists, such as thrombin or collagen, or even to higher concentrations of ADP.[16] This subtle platelet defect suggests the existence of a discrepancy that could be explained by other

Submitted May 29, 2012; accepted October 23, 2012. Prepublished online as *Blood* First Edition paper, November 13, 2012; DOI 10.1182/blood-2012-05-433730.

*R.S.R. and C.A.L. contributed equally to this study and should both be considered primary authors.

There is an Inside *Blood* commentary on this article in this issue.

The online version of this article contains a data supplement.

The publication costs of this article were defrayed in part by page charge payment. Therefore, and solely to indicate this fact, this article is hereby marked "advertisement" in accordance with 18 USC section 1734.

mechanisms, such as the contribution of Gas6 from the vasculature to thrombus formation. Thus, we hypothesize that Gas6 from the vascular wall has a role in the pathophysiology of venous thrombosis.

Methods

Animals

All experiments performed on mice were approved by the Animal Care Committee of McGill University. The *Gas6*$^{-/-}$ mice (on a C57BL/6 background) were a generous gift from Dr Peter Carmeliet (Laboratory of Angiogenesis and Neurovascular Link, Vesalius Research Center, Leuven, Belgium). The colony was maintained by the continuous crossing of *Gas6*$^{+/-}$ mice. The mice used in all experiments were male and 8-12 weeks of age. Genotyping was performed by PCR amplification of the *Gas6* gene from total genomic DNA prepared by phenol-chloroform extraction of ear punch samples. Custom primers for *Gas6* were from Invitrogen, and the nucleotide sequences are as follows: *Gas6* sense, 5′-GAGTGCCGTGATTCTGGTC-3′; *Gas6* antisense, 5′-CCACTAAGGAAACAATAACTG-3′; and *Gas6* "new," 5′-ATCTCTCGTGGGATCATT-3′.

Thermal cycling was performed on a PerkinElmer GeneAmp PCR System (2400; PerkinElmer Life and Analytical Sciences). The thermal profile was as follows: 2 minutes at 94°C, 35 cycles of: 94°C for 30 seconds, 57°C for 30 seconds, and 72°C for 30 seconds followed by a final incubation at 72°C for 10 minutes. PCR-amplified DNA was resolved on ethidium bromide-stained 1% agarose gels (Invitrogen). A single band that migrates at 500 bp corresponds to a wild-type (WT) mouse, whereas a single band of 350 bp corresponded to a *Gas6*$^{-/-}$ mouse. In heterozygous mice, both bands are present.

Venous thrombosis model

The ferric chloride ($FeCl_3$) model of thrombosis was used as previously described[18] and adapted to the inferior vena cava (IVC). Mice were anesthetized by inhalational isoflurane and placed in the supine position on a heating pad set to 37°C. After a midline laparotomy, the intestines were exteriorized and placed to the left of the animal. A piece of gauze soaked in physiologic saline was placed over the intestines to prevent desiccation. A section of IVC between the renal and left common iliac veins was cleared and separated from the aorta by dissection. A piece of Whatman filter paper (2.0×4.0 mm) was presaturated in a solution of 0.37M $FeCl_3$ (equivalent to 10% $FeCl_3$) in water and placed on the surface of the IVC such that the top of the filter paper was directly below the renal vein. The filter paper remained on the adventitial surface of the IVC for 3 minutes and was then removed. Thirty minutes after the initial application of filter paper, the clot alone or the entire section of IVC was removed for downstream processing. When the thrombus was to be weighed, it was dissected out directly from the IVC and blotted dry before weighing. Thrombi were placed in 200 μL of 100mM Tris buffer supplemented with 400 μg Proteinase K (Fermentas) for overnight digestion at 50°C for 24 hours, and total thrombus protein content was measured by reading the optical density of solutions at 280 nm.[18] Blank readings were taken as the Tris buffer and proteinase K alone.

Bone marrow transplantation

The bone marrow transplantation protocol used has been established and optimized to maximize both animal survival and ablation of recipient marrow in C57BL/6 mice.[19] All recipient mice received a total body radiation dose of 12.0 Gy (2 doses of 6.0 Gy with a 4-hour interval). Recipient male mice were anesthetized by intraperitoneal injection of rodent cocktail (ketamine, xylazine, acepromazine, 0.3 mL/25 g) before each exposure. After each exposure, mice were kept under a heating lamp for 3 hours and were given intraperitoneal injections of 1 mL warm saline to aid recovery. Recipient mice were infused with donor marrow cells 24 hours after the second exposure. The isolation of bone marrow cells was performed under sterile conditions. Donor mice were killed, and the femurs and tibias were harvested and flushed with media. The flushed marrow suspensions were centrifuged at 400*g* for 5 minutes. Erythrocytes were removed by resuspending pellets in 2 mL of red blood cell lysis buffer (Sigma-Aldrich). The cells were washed 3 times and reconstituted such that each 300-μL intravenous injection would contain 4×10^6 bone marrow cells. Recipient mice were housed in sterile cages, with antibiotic containing food and allowed 1 month for recovery and hematologic reconstitution. Success of marrow uptake was determined by *Gas6* PCR from DNA isolated from peripheral blood cells and ear punch samples. After a 1-month recovery period after irradiation, all surviving mice appeared healthy and weighed approximately the same as they did before irradiation. Survival rates per experiment ranged between 70% and 75%.

Platelet depletion/reconstitution model

To deplete endogenous platelets, mice were injected with rabbit anti–mouse thrombocyte serum (10 μL) intraperitoneally (Accurate Chemical and Scientific Corporation). Platelet depletion was allowed to proceed for 4 hours, after which a few microliters of blood were drawn from the saphenous vein of the animal and collected in EDTA-primed microvettes (Sarstedt). To confirm successful depletion of platelets, blood samples were analyzed on a Vet abc animal blood counter (Vet Novations). Platelet depletion was considered successful if the total level of circulating platelets decreased $< 120 \times 10^3/mm^3$. Mice were then reinfused with platelets collected from a donor mouse. For preparation of platelet-rich plasma, blood was collected by cardiac puncture in syringes primed with collection buffer (38mM citric acid, 75mM trisodium citrate, 100mM dextrose) from a donor mouse. Approximately 1 mL of blood was collected from each donor mouse. The blood was then diluted in one volume of wash buffer (150mM NaCl, 20mM PIPES, pH 6.5) and centrifuged for 7 minutes at 60*g*. The platelet-rich plasma was collected and centrifuged for an additional 10 minutes at 70*g*. The supernatant was removed and platelets resuspended in Walsh buffer (137mM NaCl, 20mM PIPES, 5.6mM dextrose, 1 g/L BSA, 1mM $MgCl_2$, 2.7mM KCl, 3.3mM NaH_2PO_4, pH 7.4). Purity of platelets in the platelet-rich plasma compared with whole blood was assessed by flow cytometry. Platelets were stained using CD41-PE (BD Biosciences PharMingen) and monocytes with CD14-APC (eBioscience). Platelet-rich plasma and blood were incubated with both CD41 and CD14 antibodies. Flow cytometric measurements were performed on a FACSCalibur (BD Biosciences) using CellQuest Version 4.0.2 software. Platelets and monocytes were identified based on their distinct laser scatter properties, platelets being smaller than monocytes. Two distinct populations were identified in the whole blood, whereas only the population of smaller size remained in the platelet-rich plasma. Fluorescence gating (gating on FL3/PE and FL4/APC) was done on the 2 populations. Positive staining showed 2 distinct populations in the whole blood: one $CD14^+$ and one $CD41^+$. In the platelet-rich plasma, only the $CD41^+$ population was found (supplemental Figure 1, available on the *Blood* Web site; see the Supplemental Materials link at the top of the online article).

The entirety of platelets from the donor mouse was injected into the recipient via tail vein injection. Ten minutes after the reinfusion of platelets, blood was once again collected via saphenous puncture (opposite leg) and analyzed by the blood counter. If the new circulating platelet count successfully rose to levels considered normal ($120\text{-}600 \times 10^3/mm^3$), we proceeded to challenge the mice with $FeCl_3$.

Hematoxylin and eosin and immunofluorescence staining

The venous wall with thrombi were removed, fixed in 4% paraformaldehyde for 4 hours, and incubated in PBS/30% sucrose overnight at 4°C. Samples were embedded vertically in OTC compound (Tissue-tek, Sakura), and serial 5-μm frozen sections were cut using cryostat and transferred onto gelatin-coated slides. Nonspecific binding sites on the tissues sections were blocked with 10% BSA for 30 minutes at room temperature. Thereafter, sheep anti–mouse VWF (Abcam) followed by an anti–sheep AlexaFluor 568-nm (Invitrogen) secondary antibody and rabbit anti–human fibrinogen-FITC (Dako North America) were used to visualize thrombi in the IVC. Goat anti–mouse CD31, anti–mouse α-smooth muscle actin coupled to Cy3

(Dako North America) or mouse anti–mouse TF (Santa Cruz Biotechnology) antibodies were applied, followed by appropriate secondary antibodies, AlexaFluor anti–goat 488 nm and anti–mouse 405 nm (Invitrogen). Images were acquired with a Leica DM 2000 fluorescent microscope and the Infinity Capture Version 4.6.0 software. Quantifications of TF positive staining were done using ImageJ Version 1.44p (National Institutes of Health) by delimiting the signal between luminal side of the endothelial layer and the outer side of the smooth muscle cell layer.

Isolation of endothelial cells

Endothelial cells were isolated from lungs of 8-week-old WT or *Gas6*$^{-/-}$ mice. The whole lungs were cut into small pieces with sharp scissors and incubated at 37°C for 60 minutes in 0.1% collagenase A (Roche Diagnostics) in RPMI + penicillin/streptomycin. The suspension was transferred into a 50-mL tube and passed 15 times through a 16-G needle, then through a cell strainer (100 mm) and centrifuged at 226*g* for 5 minutes. The supernatant was removed and cells plated into 75-cm^2 tissue culture flasks, coated with 0.1% gelatin and grown for 1 week in DMEM/F12 containing 20% FBS and supplemented with 20 mg/mL of endothelial cell growth serum (VWR International). Endothelial cells were purified by 2 consecutive immuno-selection procedures using magnetic beads conjugated with anti–ICAM-2 antibody (BD Biosciences PharMingen) and plated into 75-cm^2 tissue culture-coated flasks. Endothelial cells were used for experiments at passage 3. The purity of the cell preparation was evaluated by FACS and immunofluorescence. For flow cytometry analysis, cells were stained with CD31-FITC (BD Biosciences PharMingen) and propidium iodide and analyzed by flow cytometry. Propidium iodide staining allowed us to gate on live cells and from this gate, the percentage of CD31$^+$ cells was evaluated. FACS analysis showed that 87% ± 3% of the gated live cells expressed CD31 (supplemental Figure 2A). For immunofluorescence staining, cells were incubated with goat anti–mouse CD31 followed by AlexaFluor anti–goat 488 nm. Quantification of positive cells (green) over the total number of cells (4,6-diamidino-2-phenylindole, blue) showed an average of 83% ± 2% of the cells expressing CD31 (supplemental Figure 2B). For the experiments, endothelial cells were treated with vehicle, 1 U of thrombin (Haematologic Technologies), or 100 ng/mL of murine recombinant Gas6 (R&D Systems).

TF activity assay

The following protocol was adapted from Kothari et al.[20] Human blood factors factor VIIa, factor X, factor Xa, and thrombin were obtained from Haematologic Technologies. Chromogenic substrate S-2765 was obtained from diaPharma. Cells were seeded in 24-well, gelatin (1.0%)–coated plates at a density of 1×10^6 mL endothelial cells per milliliter of media. At 24 hours after seeding, the cell monolayers were washed twice in wash buffer (10mM HEPES, 0.15M NaCl, 4mM KCl, 11mM dextrose, pH 7.5) and then overlaid with 250 μL of assay buffer (10mM HEPES, 0.15M NaCl, 4mM KCl, 11mM dextrose, 5mM $CaCl_2$, 1.0 mg/mL BSA, pH 7.5) supplemented with 10nM factor VIIa. The cell monolayers were then placed at 37°C for 5 minutes to allow TF-factor VIIa complex formation; 175nM factor X was then added to each well and incubated at 37°C for 1 hour. The reaction was stopped by placing a 25 μL aliquot of reaction mixture into 50 μL of stop buffer (TBS containing 1 mg/mL BSA and 10mM EDTA). A total of 50 μL of the stopped reaction mixture was mixed with 50 μL of the chromogenic substrate S-2765 (1.7mM) and read in a microplate reader for 15 minutes at 405 nm (SpectraMax Plus 384, Molecular Devices). Final amounts of factor Xa generated were calculated using a standard curve of human factor Xa (starting from 1.0 μg/mL and diluted with of 2-fold dilution factor) versus optical density generated on a Molecular Devices plate reader, as has been previously published.[20]

Quantitative RT-PCR

Expression of TF was verified by quantitative RT-PCR. Endothelial cell RNA was isolated using an Total RNA mini kit (Froggabio) as per the manufacturer's instructions. A total of 1 μg of total RNA was reversed-transcribed with random hexamers and Superscript II (Invitrogen). Quantitative RT-PCR was performed using Fast SYBR Green master mix (Quanta Biosciences). Thermal cycling was performed with a 7500 Fast Real Time PCR System from Applied Biosystems. Each quantitative RT-PCR sample was normalized to the expression of ribosomal protein S18. Primers were designed using Primer3 (Massachusetts Institute of Technology Center for Genome Research, Cambridge, MA). Annealing temperature was 60°C. The primers sequences for murine TF and Gas6 are as follows: TF forward, 5′-CTCCTCCTCCAGGTGATCG-3′ and TF reverse, 5′-GGGTTGCCACTCCAAAATTG-3′[21]; Gas6 forward, 5′-CGAGGGGGCCTAAAACTATC-3′; and Gas6 reverse, 5′-AGGACAATCCAGGTGCTGTC-3′. Data were calculated using the ΔC_t method.

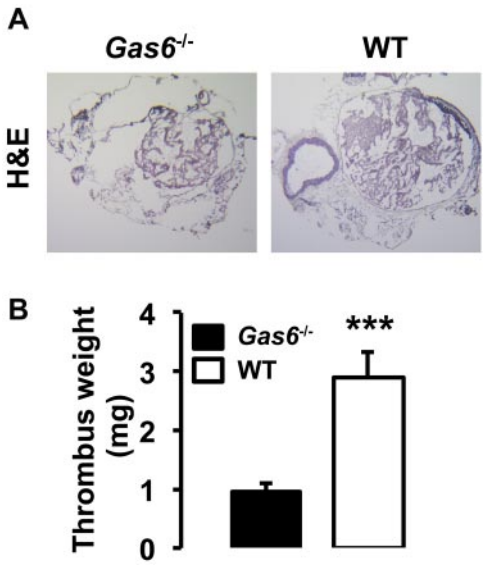

Figure 1. Inactivation of *Gas6* protect mice against venous thrombosis. (A) $FeCl_3$-induced thrombosis in the IVC of WT and *Gas6*$^{-/-}$ mice. Representative hematoxylin and eosin staining of thrombi shows that WT mice develop larger thrombi than *Gas6*$^{-/-}$ mice (original magnification ×4). (B) Quantification of thrombus weight demonstrated that thrombi from *Gas6*$^{-/-}$ mice weigh significantly less than thrombi from WT mice (n = 7). ***$P < .001$.

Statistical analysis

Data are presented as mean ± SEM. Within-group differences were assessed by 1-way ANOVA followed by a posthoc Student Newman-Keuls test. A value of $P < .05$ was considered statistically significant.

Results

Gas6 from the hematopoietic and the nonhematopoietic compartment contributes to thrombus generation

Both arterial and life-threatening thrombosis have previously been shown to be prevented in *Gas6*$^{-/-}$ mice.[16] To extend these observations to the venous system, thrombosis was induced in the IVC by applying 0.37M $FeCl_3$ to the outer adventitial layer of WT and *Gas6*$^{-/-}$ mice. After 30 minutes, thrombi were harvested and hematoxylin and eosin staining was used for visualization. Consistent with previous observations, venous thrombi from *Gas6*$^{-/-}$ mice were smaller than those from WT mice (Figure 1A). Thrombi from WT mice developed with an average weight of 2.9 mg, whereas thrombi produced in *Gas6*$^{-/-}$ mice weighed only 0.9 mg (Figure 1B). These values correspond to a 70% reduction in thrombus weight. To investigate a possible contribution of Gas6 from the vascular wall to thrombus formation, we used a bone marrow transplantation strategy to generate mice with selective ablations of *Gas6* in the nonhematopoietic or hematopoietic

compartments. For bone marrow transplantation experiments, 4 groups of mice were generated: (1) WT donor marrow into WT recipient mice (WT → WT); (2) *Gas6*$^{-/-}$ donor marrow into *Gas6*$^{-/-}$ recipient mice (*Gas6*$^{-/-}$ → *Gas6*$^{-/-}$); (3) *Gas6*$^{-/-}$ donor marrow into WT recipient mice (*Gas6*$^{-/-}$ → WT); and (4) WT donor marrow into *Gas6*$^{-/-}$ recipient mice (WT → *Gas6*$^{-/-}$). For all bone marrow transplantation experiments performed, the success of marrow uptake was verified. DNA was extracted from ear punch samples (nonhematopoietic) and blood (hematopoietic) before and after bone marrow transplantation. Successful bone marrow transplantation experiments are evidenced in lanes 3 and 6 of an agarose gel showing a DNA staining pattern consistent with a *Gas6*$^{-/-}$ phenotype in the hematopoietic compartment of 2 recipient WT mice after irradiation and transplantation with *Gas6*$^{-/-}$ bone marrow (Figure 2A). After $FeCl_3$ injury, we found that clots from *Gas6*$^{-/-}$ → *Gas6*$^{-/-}$ mice were significantly smaller than clots from WT → WT mice. Interestingly, thrombi from chimeric mice (*Gas6*$^{-/-}$ → WT and WT → *Gas6*$^{-/-}$) were of intermediate size (ie, smaller than those from WT → WT mice, but larger than the ones from *Gas6*$^{-/-}$ → *Gas6*$^{-/-}$ mice; Figure 2B). Then, total thrombus protein content was determined, a parameter that, like the thrombus weight, reflects thrombus size. Thrombus protein content from WT → WT mice was significantly higher than from the *Gas6*$^{-/-}$ → *Gas6*$^{-/-}$ mice (Figure 2C). Given the intermediate phenotype of the chimeric mice, these data suggest that Gas6 from both hematopoietic and nonhematopoietic cells contributes to thrombus formation.

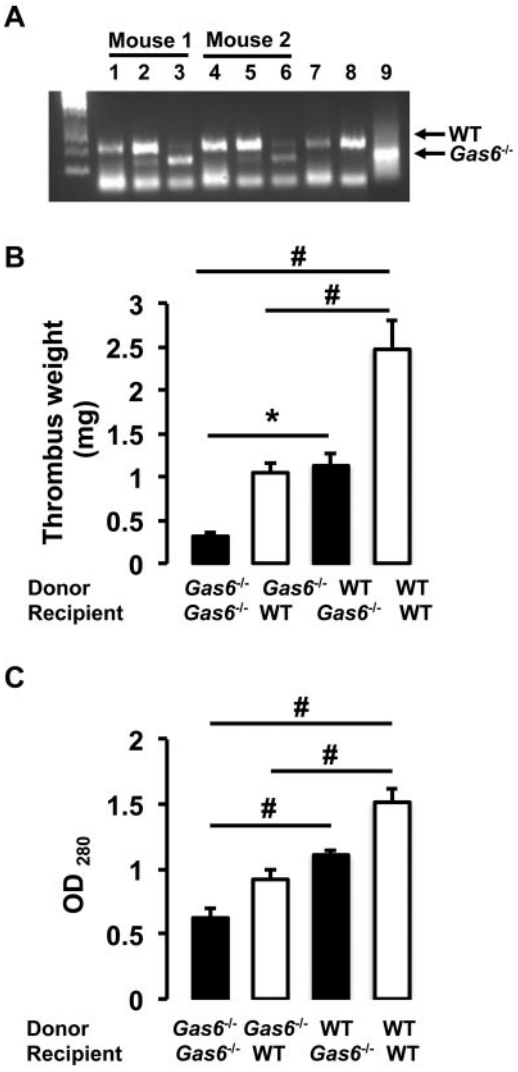

Figure 2. Contribution of vascular Gas6 to thrombus generation. (A) Success of marrow uptake after irradiation/transplantation was determined by *Gas6* PCR from DNA isolated from peripheral blood cells (hematopoietic) and ear (nonhematopoietic). Lanes 1 and 4 indicate nonhematopoietic DNA from ears of WT mouse before transplantation; lanes 2 and 5, DNA from ears of WT mouse transplanted with bone marrow from *Gas6*$^{-/-}$ mice; lanes 3 and 6, hematopoietic DNA from blood of WT mice transplanted with bone marrow from *Gas6*$^{-/-}$ mice; lane 7, DNA from blood of a WT mouse transplanted with bone marrow from a WT mouse; lane 8, DNA from the ear of a WT mouse; and lane 9, DNA from the ear of a *Gas6*$^{-/-}$ mouse. (B) Thrombosis was induced in the 4 groups of mice generated by the bone marrow transplantation experiments. Thrombus weight from chimeric mice (*Gas6*$^{-/-}$ → WT and WT → *Gas6*$^{-/-}$) had an intermediate weight compared with *Gas6*$^{-/-}$ → *Gas6*$^{-/-}$ and WT → WT (n = 8). *$P < .05$. #$P < .001$. (C) Thrombi were also digested in proteinase K. Protein concentration evaluation confirmed the intermediate phenotype of chimeric mice (n = 8). #$P < .001$.

Contribution of platelet and vascular cells Gas6 to thrombus formation in vivo

Because *Gas6*$^{-/-}$ mice have been described to have mainly a platelet defect, we evaluated the contribution of platelets alone, in contrast to the bone marrow transplantation experiments from the previous paragraph that examined the entire bone marrow.[16] To address this issue, we used a platelet depletion/reconstitution model to examine thrombus formation in vivo in different cohort of mice (WT → WT, *Gas6*$^{-/-}$ → WT, WT → *Gas6*$^{-/-}$, and *Gas6*$^{-/-}$ → *Gas6*$^{-/-}$). In all groups, venous thrombosis was induced with 0.37M $FeCl_3$. Platelet counts were equivalent in the whole blood of WT and *Gas6*$^{-/-}$ mice before manipulation (Figure 3A). Both WT and *Gas6*$^{-/-}$ mice were rendered thrombocytopenic and reconstituted with donor platelets. Platelets were prepared from platelet-rich plasma. The purity of the platelet preparation was ascertained by flow cytometry before injection to the recipient animal (supplemental Figure 1). Before the injection of platelets and at death, successful platelet depletion and reconstitution were verified in recipient WT and *Gas6*$^{-/-}$ mice (Figure 3B).

After induction of thrombosis in the IVC, thrombus weight was evaluated in the 4 groups of mice. We found that chimeric mice (WT mice with *Gas6*$^{-/-}$ platelets or *Gas6*$^{-/-}$ mice with WT platelets) developed thrombi of intermediate size compared with WT → WT and *Gas6*$^{-/-}$ → *Gas6*$^{-/-}$ mice. Hence, *Gas6*$^{-/-}$ → WT and WT → *Gas6*$^{-/-}$ had significantly smaller clots than WT → WT (Figure 3C). Thrombi, from WT or *Gas6*$^{-/-}$ mice rendered thrombocytopenic and reconstituted with platelets from WT or *Gas6*$^{-/-}$ mice, were prepared for hematoxylin and eosin and immunofluorescence staining. Hematoxylin and eosin was used to stain the "red" part of the thrombus enriched with red blood cells and fibrin. Hematoxylin and eosin staining showed larger thrombi in WT → WT compared with *Gas6*$^{-/-}$ →*Gas6* $^{-/-}$ mice, whereas thrombi were of intermediate size for the chimeric groups. Specific fibrin and VWF staining in the thrombus showed reduced fluorescence in *Gas6*$^{-/-}$ → WT or WT → *Gas6*$^{-/-}$ compared with WT → WT animals (Figure 4).

Gas6 up-regulates vascular TF expression and activity

We examined the possibility that Gas6's vascular effect on thrombosis could be related to expression of TF. Staining for TF (blue) was differentially colocalized with both endothelial cells (green) and smooth muscle cells (red) in the 4 groups of mice (Figure 5A). Quantifications of TF staining, in the area delimited by endothelial and smooth muscle cells, demonstrated that TF expression was significantly reduced in the vein wall of *Gas6*$^{-/-}$ → *Gas6*$^{-/-}$

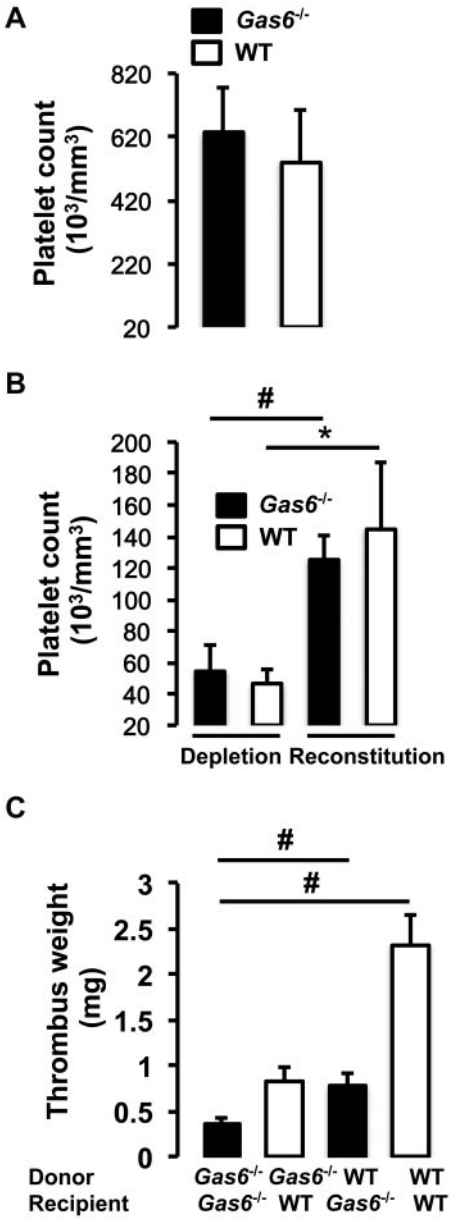

Figure 3. Equal contribution of platelets and vascular Gas6 to thrombus generation. (A) Platelet counts were equivalent in whole blood drawn from WT and *Gas6*$^{-/-}$ mice. (B) Platelet depletion was achieved by injection of rabbit anti–mouse thrombocyte serum. Platelet counts were successfully reduced by injection of rabbit anti–mouse thrombocyte serum and successfully restored after injection of platelets from a donor mouse to thrombocytopenic mice (n = 4). *$P < .05$, WT depleted versus WT reconstituted. #$P < .05$, *Gas6*$^{-/-}$ depleted versus *Gas6*$^{-/-}$ reconstituted. (C) Thrombosis was induced in the 4 groups of mice generated by the platelet depletion/reconstitution as indicated in the figure. WT or *Gas6*$^{-/-}$ mice receiving *Gas6*$^{-/-}$ or WT platelets, respectively, had thrombi of intermediate weight, similar to the results the bone marrow transplantation experiments (n = 4 or 5). #$P < .001$.

compared with WT → WT (Figure 5B). Although not statistically different, expression level of TF in *Gas6*$^{-/-}$ → WT or WT → *Gas6*$^{-/-}$ was intermediate between the 2 control groups (*Gas6*$^{-/-}$ → *Gas6*$^{-/-}$ and WT → WT; Figure 5B).

In vitro, endothelial cells extracted from WT and *Gas6*$^{-/-}$ mice were treated with thrombin, used as a prothrombotic stimulus, for 4 hours. We measured the TF/factor VIIa-dependent generation of factor Xa in endothelial cells from WT and *Gas6*$^{-/-}$ mice. Factor Xa generation was significantly reduced in *Gas6*-deficient endothelial cells compared with WT cells demonstrating reduced functional TF activity (Figure 6A). To further characterize the role of Gas6 in TF expression, endothelial cells were treated with thrombin, murine recombinant Gas6, or both. In WT cells, thrombin increases TF mRNA expression. In contrast, TF mRNA expression was blunted in *Gas6*$^{-/-}$ cells after thrombin stimulation. More importantly, when incubated with thrombin and recombinant Gas6, TF mRNA expression was increased in *Gas6*$^{-/-}$ cells to a level comparable with the WT endothelial cells (Figure 6B). One possible mechanism of a thrombin and Gas6 synergistic effect on TF expression is that thrombin induces expression and/or secretion of *Gas6*. We found that thrombin significantly increased the mRNA expression of *Gas6* in WT endothelial cells (Figure 6C).

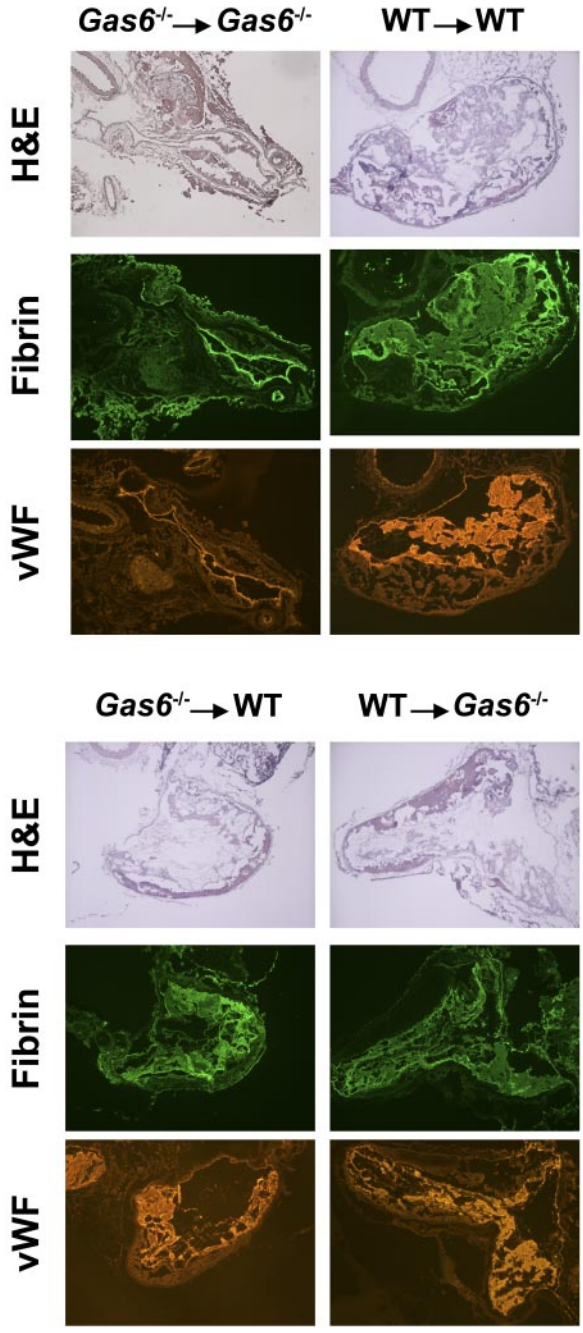

Figure 4. Hematoxylin and eosin staining and immunofluorescence analysis demonstrated that thrombi from chimeric mice had intermediate amounts of fibrin and VWF compared with *Gas6*$^{-/-}$ → *Gas6*$^{-/-}$ and WT → WT. Original magnification ×4.

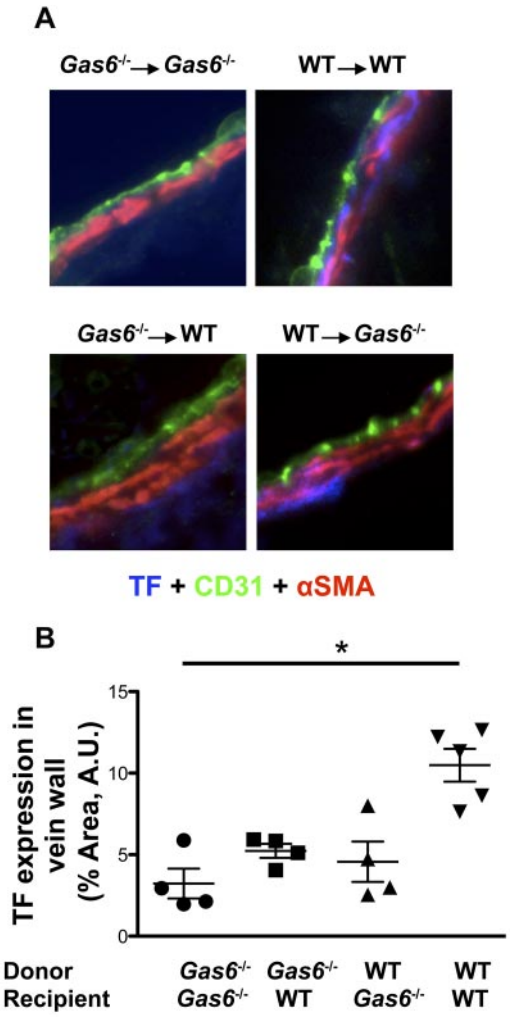

Figure 5. $FeCl_3$-induced thrombosis increased expression of TF in WT but not in *Gas6*$^{-/-}$ mice. (A) Representative immunofluorescence staining for TF in the IVC of the 4 groups of mice generated by the platelet depletion/reconstitution experiments (original magnification ×40). Endothelial cells were stained using CD31-AlexaFluor 488-nm antibodies (green). Smooth muscle cells were stained with α-smooth muscle actin (αSMA) antibody coupled with Cy3 dye (red). TF was stained with a specific primary antibody followed by AlexaFluor 405-nm (blue). (B) Quantifications of TF expression were done in the vascular wall, delimited by the endothelial cells and the smooth muscle cells. TF expression was decreased in the vascular wall of the *Gas6*$^{-/-}$ → *Gas6*$^{-/-}$ group compared with the WT → WT. Interestingly, expression of TF was intermediate in the 2 chimeric groups but not statistically different from the *Gas6*$^{-/-}$ → *Gas6*$^{-/-}$ or WT → WT groups (n = 4 or 5 per group). *$P < .05$.

Discussion

The present study demonstrates that *Gas6* deficiency in hematopoietic and nonhematopoietic compartments contributes to venous thrombus formation. More importantly, we show, for the first time, that Gas6 is required for the up-regulation of expression and activity of TF in vascular cells.

Gas6 is known for its role in other disorders of the circulatory system. For example, Gas6 is pro-atherogenic in both mice and humans[22,23] and has the potential to stimulate erythropoesis in anemic mice who have become hyporesponsive to erythropoietin treatment.[24] Angelillo-Scherrer et al described the phenotype of the *Gas6* null mice and showed that these mice are protected against lethal thromboembolism.[16] In this study, thrombosis was induced by ligation of the abdominal caval vein. *Gas6*$^{-/-}$ thrombi were 85% smaller compared with WT mice. They demonstrated that Gas6 amplified platelet aggregation and that platelet dysfunction in *Gas6*$^{-/-}$ mice resembled that of patients with platelet signaling transduction defects. However, although the *Gas6*$^{-/-}$ mice remained protected against a number of thrombosis models, reduced aggregation of platelets was observed in response to 5.0μM ADP or 10μM of the thromboxane analog U46619. Thus, there seems to be a discrepancy between this subtle defect in platelet response and the dramatic clinical phenotype observed.[16] We hypothesize that this discrepancy could be explained by a contribution of a nonhematopoietic source of Gas6, such as the vascular wall (ie, endothelial and smooth muscle cells). The role of Gas6 in human platelets and plasma also remains controversial. One study found that Gas6 was undetectable in human platelets[25]; however, more recently, it has become apparent that this might not be the case.[26] Plasma Gas6 does not have an effect on platelet aggregation.[11,27,28] However, we recently showed that elevated Gas6 plasma levels

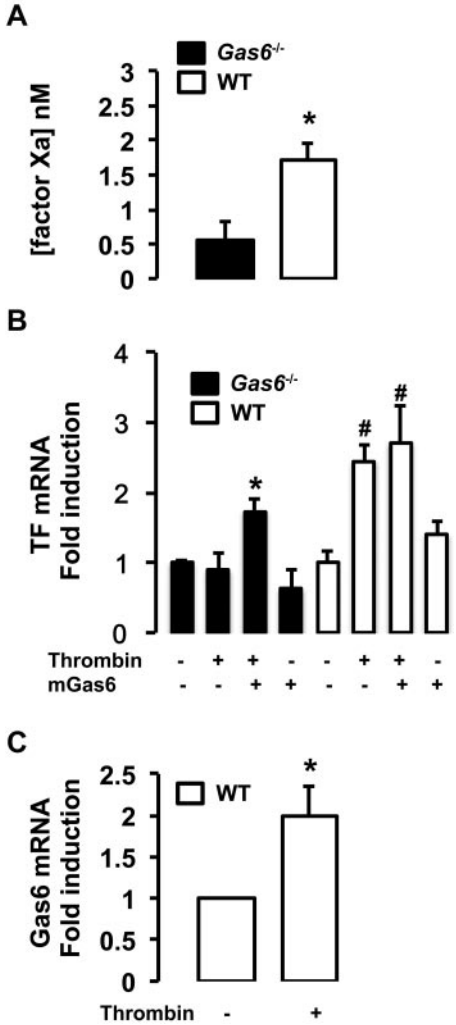

Figure 6. Decreased expression and activity of TF in *Gas6*$^{-/-}$ endothelial cells. (A) In vitro, low TF activity was also found in the media of *Gas6*$^{-/-}$ endothelial cells compared with WT cells (n = 6-8). *$P < .05$. (B) Quantitative PCR showed that TF mRNA expression was low in *Gas6*$^{-/-}$ deficient endothelial cells compared with WT. Thrombin treatment increased significantly TF mRNA expression in WT but not in *Gas6*$^{-/-}$ cells. When *Gas6*$^{-/-}$ cells were treated with both thrombin and murine recombinant Gas6, TF mRNA expression was increased to a level comparable with WT cells. Murine recombinant Gas6 alone has no significant effect on TF mRNA expression in WT or *Gas6*$^{-/-}$ cells (n = 4-10). *$P < .05$ vs *Gas6*$^{-/-}$ untreated cells. #$P < .05$ vs untreated WT cells. (C) Thrombin induced Gas6 mRNA in WT endothelial cells (n = 4-8). *$P < .05$.

were associated with venous thrombosis in humans.[29] Gas6 has already been shown to mediate different effects in the vascular system. For example, our laboratory and others have demonstrated that interactions between Gas6 and its receptor, Axl, promote endothelial cell survival through classic intracellular survival pathways.[30-32] Therefore, it is possible that Gas6 mediates its prothrombotic phenotype via the endothelial cell. Indeed, Gas6 also contributes to activation of the endothelium during inflammation[33] and has an antiapoptotic role in cultured endothelium.[30,31,34,35] Tjwa et al have demonstrated that, when stimulated with TNF-α, endothelial cells from *Gas6*$^{-/-}$ mice expressed less VCAM-1 and ICAM-1 compared with WT endothelial cells.[33] The capacity of endothelial cells to interact with platelet and leukocytes was significantly reduced in cells deficient in *Gas6*.[33] Gas6 has also been shown to play an important role in vascular smooth muscle cells. Gas6 regulates smooth muscle cell survival, migration, and proliferation, which have been demonstrated to be important in the context of restenosis after angioplasty.[27,36]

The understanding of the biologic events associated with venous thrombosis and their manipulation by pharmacologic agents are dependent on studying animal models. The $FeCl_3$ model of vessel injury, although traditionally used in arterial model of thrombosis, has recently emerged as applicable for use in veins.[18,37] We were able to successfully reproduce the *Gas6*$^{-/-}$ phenotype using the $FeCl_3$ venous thrombosis model that had not previously been used to study *Gas6*$^{-/-}$ mice. In agreement with the study from Angelillo-Scherrer et al, we found that, compared with WT mice, $FeCl_3$-induced thrombi from *Gas6*$^{-/-}$ were 70% smaller.[16] The bone marrow transplantation approach allowed us to study thrombosis in mice with selective ablations of *Gas6* in hematopoietic or nonhematopoietic compartments. The thrombus weights obtained were similar in chimeric mice and were of intermediate weights between WT → WT and *Gas6*$^{-/-}$ → *Gas6*$^{-/-}$ animals, which suggested a contribution to thrombus formation by Gas6 from a source other than the hematopoietic compartment (ie, platelets and leukocytes), possibly vascular cells (ie, endothelial and smooth muscle cells).[38] Thrombi from *Gas6*$^{-/-}$ → WT mice were of comparable weight to those produced in WT → *Gas6*$^{-/-}$ mice and raised the possibility of an approximately equal contribution by Gas6 from hematopoietic and nonhematopoietic compartments to thrombus formation. We also used a model of platelet depletion/reconstitution to create chimeric mice that lacked either platelet Gas6 only, vascular cell Gas6 only, both platelet and vascular cell Gas6, or neither.[39] This approach offers the advantage of performing the experiment on the same day without waiting 4 weeks for successful bone marrow reconstitution and avoids the inherent problem of thrombus instability after irradiation.[39] We found that chimeric mice have thrombus of intermediate size between WT → WT and *Gas6*$^{-/-}$ → *Gas6*$^{-/-}$ animals. Our results demonstrated the crucial role of Gas6 from the vascular wall in venous thrombus formation and strongly suggest an equal contribution of the nonhematopoietic and hematopoietic compartments. Interestingly, using a model of flow restriction, a recent study suggested a role for other cells from the hematopoietic compartment, such as leukocytes and neutrophils, in the initiation and propagation of venous thrombosis in association with the platelet.[40] In the present study, we found similar results regarding the thrombus weight from both the bone marrow transplantation and the platelet depletion/reconstitution models. This observation would favor a role for only the platelet, but we cannot rule out a role for leukocytes in the formation of thrombi.

Through its ability to express procoagulants and anticoagulants, as well as key cell adhesion molecules, the endothelium has emerged as one of the pivotal regulators of hemostasis. However, during states of endothelial disturbances, whether physical (eg, vascular trauma) or functional (eg, sepsis), a prothrombotic state is supported by the endothelial surface. Production of VWF, TF, plasminogen activator inhibitor-1, and factor V augment thrombosis. In addition, in response to endothelial injury, endothelial cells are activated, resulting in increased surface expression of certain cell adhesion molecules (such as P-selectin or E-selectin), promoting the adhesion and activation of platelets. This event initiates and amplifies thrombosis.[2] In a rat model of IVC ligation, TF staining was observed in both leukocytes and endothelial cells associated with the clot.[41] Thus, we investigated TF as a possible downstream molecule of the Gas6 pathway in the vascular wall. Others have suggested, but not established, that Gas6 regulates TF expression.[17] TF plays a key role in different murine models of thrombosis, including the $FeCl_3$ injury models.[24,42] The source of TF in venous thrombosis, whether produced from the endothelium, vascular smooth muscle, circulating cells, or microparticles, is still under debate.[43-45] Here we show that TF is up-regulated in the vascular wall in $FeCl_3$-induced venous thrombosis. We isolated endothelial cells from mouse lung tissue and used thrombin as a procoagulant stimulus. We found that endothelial cells isolated from *Gas6*$^{-/-}$ mice had a significantly lower pool of active TF on the surface compared with WT cells. At the level of mRNA, thrombin-induced up-regulation of TF mRNA was significantly reduced in *Gas6*$^{-/-}$ cells, indicating that these cells are hyporesponsive to endothelial activation by thrombin, which is consistent with other published observations.[33] Interestingly, we found that treatment of *Gas6*$^{-/-}$ endothelial cells with thrombin and murine recombinant Gas6 restored TF mRNA expression to levels comparable with WT cells incubated with the same reagents. Thus, one can speculate that thrombin induces the secretion of Gas6, possibly through de novo protein synthesis. Then, binding of Gas6 to its receptor Axl might lead to the expression of TF. We found that thrombin induces Gas6 mRNA expression in WT endothelial cells. Thus, these results suggested that thrombin might be involved in the secretion of Gas6. Taken together, the data presented here provide evidence that Gas6 positively regulates TF expression in murine endothelial cells and could, in part, explain how Gas6 contributes to thrombus formation in vivo.

Acknowledgments

This work was supported by the Canadian Institutes for Health Research (M.D.B.; team grant in venous thromboembolism; Dr J. Weitz, Principal Investigator) and the Heart and Stroke Foundation (Grant-in-aid; M.D.B.).

Authorship

Contribution: R.S.R. designed the experiments of bone marrow transplantation and TF activity assay, performed research, and analyzed the data; C.A.L. designed experiments of platelet depletion/reconstitution, immunofluorescence, and real-time quantitative PCR, performed research, analyzed the data, and wrote the manuscript; S.L., M.N.A., and J.W. performed research; and M.D.B. conceived and financed the study and wrote the manuscript.

Conflict-of-interest disclosure: The authors declare no competing financial interests.

Correspondence: Mark D. Blostein, Lady Davis Institute for Medical Research, McGill University, 3999 Côte-Ste-Catherine Road, Room F-130, Montreal, QC, Canada, H3T 1E2; e-mail: mark.blostein@mcgill.ca.

References

1. Sevitt S. The structure and growth of valve-pocket thrombi in femoral veins. *J Clin Pathol.* 1974;27(7):517-528.
2. Wakefield TW, Myers DD, Henke PK. Mechanisms of venous thrombosis and resolution. *Arterioscler Thromb Vasc Biol.* 2008;28(3):387-391.
3. Becker BF, Heindl B, Kupatt C, Zahler S. Endothelial function and hemostasis. *Z Kardiol.* 2000; 89(3):160-167.
4. Hafizi S, Dahlback B. Gas6 and protein S: vitamin K-dependent ligands for the Axl receptor tyrosine kinase subfamily. *FEBS J.* 2006;273(23):5231-5244.
5. Stitt TN, Conn G, Gore M, et al. The anticoagulation factor protein S and its relative, Gas6, are ligands for the Tyro 3/Axl family of receptor tyrosine kinases. *Cell.* 1995;80(4):661-670.
6. Godowski PJ, Mark MR, Chen J, Sadick MD, Raab H, Hammonds RG. Reevaluation of the roles of protein S and Gas6 as ligands for the receptor tyrosine kinase Rse/Tyro 3. *Cell.* 1995;82(3):355-358.
7. Manfioletti G, Brancolini C, Avanzi G, Schneider C. The protein encoded by a growth arrest-specific gene (gas6) is a new member of the vitamin K-dependent proteins related to protein S, a negative coregulator in the blood coagulation cascade. *Mol Cell Biol.* 1993;13(8):4976-4985.
8. Nakano T, Higashino K, Kikuchi N, et al. Vascular smooth muscle cell-derived, Gla-containing growth-potentiating factor for $Ca^{(2+)}$-mobilizing growth factors. *J Biol Chem.* 1995;270(11):5702-5705.
9. Avanzi GC, Gallicchio M, Cavalloni G, et al. GAS6, the ligand of Axl and Rse receptors, is expressed in hematopoietic tissue but lacks mitogenic activity. *Exp Hematol.* 1997;25(12):1219-1226.
10. Fernandez-Fernandez L, Bellido-Martin L, Garcia de Frutos P. Growth arrest-specific gene 6 (GAS6): an outline of its role in haemostasis and inflammation. *Thromb Haemost.* 2008;100(4):604-610.
11. Ekman C, Linder A, Akesson P, Dahlback B. Plasma concentrations of Gas6 (growth arrest specific protein 6) and its soluble tyrosine kinase receptor sAxl in sepsis and systemic inflammatory response syndromes. *Crit Care.* 2010;14(4): R158.
12. Llacuna L, Barcena C, Bellido-Martin L, et al. Growth arrest-specific protein 6 is hepatoprotective against murine ischemia/reperfusion injury. *Hepatology.* 2010;52(4):1371-1379.
13. Yanagita M. The role of the vitamin K-dependent growth factor Gas6 in glomerular pathophysiology. *Curr Opin Nephrol Hypertens.* 2004;13(4): 465-470.
14. Yagami T, Ueda K, Asakura K, et al. Gas6 rescues cortical neurons from amyloid beta protein-induced apoptosis. *Neuropharmacology.* 2002; 43(8):1289-1296.
15. Funakoshi H, Yonemasu T, Nakano T, Matumoto K, Nakamura T. Identification of Gas6, a putative ligand for Sky and Axl receptor tyrosine kinases, as a novel neurotrophic factor for hippocampal neurons. *J Neurosci Res.* 2002;68(2):150-160.
16. Angelillo-Scherrer A, de Frutos P, Aparicio C, et al. Deficiency or inhibition of Gas6 causes platelet dysfunction and protects mice against thrombosis. *Nat Med.* 2001;7(2):215-221.
17. Angelillo-Scherrer A, Burnier L, Flores N, et al. Role of Gas6 receptors in platelet signaling during thrombus stabilization and implications for antithrombotic therapy. *J Clin Invest.* 2005;115(2): 237-246.
18. Wang X, Smith PL, Hsu MY, Ogletree ML, Schumacher WA. Murine model of ferric chloride-induced vena cava thrombosis: evidence for effect of potato carboxypeptidase inhibitor. *J Thromb Haemost.* 2006;4(2):403-410.
19. Cui YZ, Hisha H, Yang GX, et al. Optimal protocol for total body irradiation for allogeneic bone marrow transplantation in mice. *Bone Marrow Transplant.* 2002;30(12):843-849.
20. Kothari H, Kaur G, Sahoo S, Idell S, Rao LV, Pendurthi U. Plasmin enhances cell surface tissue factor activity in mesothelial and endothelial cells. *J Thromb Haemost.* 2009;7(1):121-131.
21. Ganopolsky JG, Castellino FJ. A protein C deficiency exacerbates inflammatory and hypotensive responses in mice during polymicrobial sepsis in a cecal ligation and puncture model. *Am J Pathol.* 2004;165(4):1433-1446.
22. Lutgens E, Tjwa M, Garcia de Frutos P, et al. Genetic loss of Gas6 induces plaque stability in experimental atherosclerosis. *J Pathol.* 2008; 216(1):55-63.
23. Tjwa M, Moons L, Lutgens E. Pleiotropic role of growth arrest-specific gene 6 in atherosclerosis. *Curr Opin Lipidol.* 2009;20(5):386-392.
24. Angelillo-Scherrer A, Burnier L, Lambrechts D, et al. Role of Gas6 in erythropoiesis and anemia in mice. *J Clin Invest.* 2008;118(2):583-596.
25. Balogh I, Hafizi S, Stenhoff J, Hansson K, Dahlbäck B. Analysis of Gas6 in human platelets and plasma. *Arterioscler Thromb Vasc Biol.* 2005; 25(6):1280-1286.
26. Cosemans JM, Van Kruchten R, Olieslagers S, et al. Potentiating role of Gas6 and Tyro3, Axl and Mer (TAM) receptors in human and murine platelet activation and thrombus stabilization. *J Thromb Haemost.* 2010;8(8):1797-1808.
27. Clauser S, Bachelot-Lozat C, Fontana P, et al. Physiological plasma Gas6 levels do not influence platelet aggregation. *Arterioscler Thromb Vasc Biol.* 2006;26(3):e22.
28. Burnier L, Borgel D, Angelillo-Scherrer A, Fontana P. Plasma levels of the growth arrest-specific gene 6 product (Gas6) and antiplatelet drug responsiveness in healthy subjects. *J Thromb Haemost.* 2006;4(10): 2283-2284.
29. Blostein MD, Rajotte I, Rao DP, Holcroft CA, Kahn SR. Elevated plasma gas6 levels are associated with venous thromboembolic disease. *J Thromb Thrombolysis.* 2011;32(3):272-278.
30. Hasanbasic I, Cuerquis J, Varnum B, Blostein MD. Intracellular signaling pathways involved in Gas6-Axl-mediated survival of endothelial cells. *Am J Physiol Heart Circ Physiol.* 2004;287(3):H1207-H1213.
31. Hasanbasic I, Rajotte I, Blostein M. The role of gamma-carboxylation in the anti-apoptotic function of gas6. *J Thromb Haemost.* 2005;3(12): 2790-2797.
32. Healy AM, Schwartz JJ, Zhu X, Herrick BE, Varnum B, Farber HW. Gas 6 promotes Axl-mediated survival in pulmonary endothelial cells. *Am J Physiol Lung Cell Mol Physiol.* 2001;280(6): L1273-L1281.
33. Tjwa M, Bellido-Martin L, Lin Y, et al. Gas6 promotes inflammation by enhancing interactions between endothelial cells, platelets, and leukocytes. *Blood.* 2008;111(8):4096-4105.
34. O'Donnell K, Harkes IC, Dougherty L, Wicks IP. Expression of receptor tyrosine kinase Axl and its ligand Gas6 in rheumatoid arthritis: evidence for a novel endothelial cell survival pathway. *Am J Pathol.* 1999;154(4):1171-1180.
35. Ganopolsky JG, Abid MR, Aird WC, Blostein MD. GAS6-induced signaling in human endothelial cells is mediated by FOXO1a. *J Thromb Haemost.* 2008;6(10):1804-1811.
36. Melaragno MG, Cavet ME, Yan C, et al. Gas6 inhibits apoptosis in vascular smooth muscle: role of Axl kinase and Akt. *J Mol Cell Cardiol.* 2004; 37(4):881-887.
37. Diaz JA, Obi AT, Myers DD Jr, et al. Critical review of mouse models of venous thrombosis. *Arterioscler Thromb Vasc Biol.* 2012;32(3):556-562.
38. Laurance S, Lemarie CA, Blostein MD. Growth arrest-specific gene 6 (gas6) and vascular hemostasis. *Adv Nutr.* 2012;3(2):196-203.
39. Orlowski E, Chand R, Yip J, et al. A platelet tetraspanin superfamily member, CD151, is required for regulation of thrombus growth and stability in vivo. *J Thromb Haemost.* 2009;7(12): 2074-2084.
40. von Bruhl ML, Stark K, Steinhart A, et al. Monocytes, neutrophils, and platelets cooperate to initiate and propagate venous thrombosis in mice in vivo. *J Exp Med.* 2012;209(4):819-835.
41. Zhou J, May L, Liao P, Gross PL, Weitz JI. Inferior vena cava ligation rapidly induces tissue factor expression and venous thrombosis in rats. *Arterioscler Thromb Vasc Biol.* 2009;29(6):863-869.
42. Wang L, Miller C, Swarthout RF, Rao M, Mackman N, Taubman MB. Vascular smooth muscle-derived tissue factor is critical for arterial thrombosis after ferric chloride-induced injury. *Blood.* 2009;113(3):705-713.
43. Day SM, Reeve JL, Pedersen B, et al. Macrovascular thrombosis is driven by tissue factor derived primarily from the blood vessel wall. *Blood.* 2005; 105(1):192-198.
44. Tesselaar ME, Romijn FP, Van Der Linden IK, Prins FA, Bertina RM, Osanto S. Microparticle-associated tissue factor activity: a link between cancer and thrombosis? *J Thromb Haemost.* 2007;5(3):520-527.
45. de Waard V, Hansen HR, Spronk HH, et al. Differential expression of tissue factor mRNA and protein expression in murine sepsis: the role of the granulocyte revisited. *Thromb Haemost.* 2006; 95(2):348-353.